



4<sup>th</sup> IASPEI / IAEE International Symposium:

## Effects of Surface Geology on Seismic Motion

August 23–26, 2011 • University of California Santa Barbara

### ESTIMATION OF INTERSTATION GREEN'S FUNCTIONS IN THE LONG-PERIOD RANGE (2-10S) FROM CONTINUOUS RECORDS OF F-NET BROADBAND SEISMOGRAPH NETWORK IN SOUTHWESTERN JAPAN

**Kimiyuki ASANO**

Disaster Prevention Research Institute  
Kyoto University  
Uji, Kyoto 611-0011  
Japan

**Asako IWAKI**

National Research Institute for  
Earth Science and Disaster Prevention  
Tsukuba, Ibaraki 305-0006  
Japan

**Tomotaka IWATA**

Disaster Prevention Research Institute  
Kyoto University  
Uji, Kyoto 611-0011  
Japan

#### ABSTRACT

We applied the seismic interferometry to the whole-year continuous records from 24 F-net broadband stations of NIED in southwestern Japan. We extracted the interstation Green's functions by taking the cross-correlations of 211 station-pairs whose interstation distances are less than 400 km. The one-bit normalization is used to suppress the nonstationary signals. The Rayleigh-wave type signal which propagates according to the interstation distance is recognized from this result. The group velocities in the period range between 2 and 10 s are estimated for all station-pairs by the multiple filter analyses. In northern region the estimated group velocity is faster than the southern region, which suggests the difference of shear-wave velocity in the surface layers between these regions. Then, we compared the observed interstation Green's functions with the theoretical Green's functions calculated from the three-dimensional crustal velocity model, which was proposed for ground motion prediction by compiling seismological information by Iwata *et al.* [2008], to validate and update the model. This three-dimensional velocity model is composed of 9 homogeneous layers including subducting slab. We are improving the velocity model by comparing the simulated and observed interstation Green's functions including the regional dependence on *P*- and *S*-wave velocities in the uppermost layer.

#### INTRODUCTION

The interstation Green's function can be extracted by stacking correlations of diffuse wave fields recorded at two stations over large amount of data. This technique is widely applied to seismic coda (e.g., Campillo and Paul, 2003; Snieder, 2004) and ambient seismic noise records (e.g., Shapiro and Campillo, 2004; Sabra *et al.*, 2005; Bensen *et al.*, 2007; Yamanaka *et al.*, 2010). Shapiro and Campillo [2004] demonstrated that the coherent broadband Rayleigh waves could be extracted from the ambient seismic noise by computing cross-correlations of vertical component records of several days of seismic noise at different pairs of stations separated by distances from about 100 to 2000 km.

On the strong ground motion prediction for future earthquakes, it is essential to develop the reliable crustal velocity structure models along the propagation path from the source to the target area. As for southwestern Japan, where the Philippines Sea Plate subducts beneath the Eurasia Plate, mega-thrust earthquakes called Tonankai and Nankai earthquakes are expected to occur along the Nankai trough with high probability (Headquarters for Earthquake Research Promotion, 2011). It is an urgent issue to predict long-period ground motions in the sedimentary basins distributed over southwestern Japan for such mega thrust earthquakes. Recently, Iwata *et al.* [2008] has constructed the three-dimensional crustal and basin velocity structure models for ground motion prediction for future crustal and subduction earthquakes in southwestern Japan, and their models have been used for ground motion simulation studies (e.g., Iwaki *et al.*, 2009). They constructed these models by compiling a number of geophysical exploration results such as reflection profiles, receiver function profiles, seismic tomography, and etc. We have to make constant efforts to validate how the existing three-dimensional velocity structure models will explain the observed waveforms by performing ground motion simulations in the target periods. The observed seismograms from large to moderate earthquakes, which have enough signal-to-noise ratios in the long-period

range (ex. 2-10 s), are usually used for ground motion simulations. However, such hypocenters are not always uniformly distributed around the target region, and large events bringing a number of data with good signal-to-noise ratios do not occur very frequently.

The interstation Green's function extracted from the ambient seismic noise fields recorded by the dense seismic network might enable us to obtain useful data set for this kind of study, because ambient noise does not depend on the seismicity in the target region. For example, Ma *et al.* [2008] extracted interstation Green's functions by correlating the vertical component of ambient seismic noise recorded at 56 broadband stations with dense coverage in the greater Los Angeles area, and they tested two community velocity models (CVM 4.0 and CVM-H 5.2) developed by the Southern California Earthquake Center (SCEC) by comparing the observed interstation Green's functions with those calculated by the finite element method.

In this paper, the interstation Green's functions are estimated from the whole-year continuous records of 24 broadband seismic stations in southwestern Japan to obtain the quantitative information on the wave propagation characteristics in the long-period range (2–10s) for testing the present three-dimensional crustal structure model in this area.

## ESTIMATION OF INTERSTATION GREEN'S FUNCTIONS FROM BROADBAND NOISE DATA

### Theoretical background

The cross-correlation of the velocity wavefields at two stations  $\mathbf{x}_A$  and  $\mathbf{x}_B$  can be written as the superposition of the causal and anti-causal velocity Green's functions (e.g., Wapenaar and Fokkema, 2006),

$$\langle C_{qp}^{vel}(\mathbf{x}_B, \mathbf{x}_A, t) \rangle \approx \left\{ \dot{G}_{qp}(\mathbf{x}_B, \mathbf{x}_A, t) + \dot{G}_{qp}(\mathbf{x}_B, \mathbf{x}_A, -t) \right\}^* S(t), \quad (1)$$

where the  $\dot{G}_{qp}(\mathbf{x}_B, \mathbf{x}_A, t)$  is the time derivative of the Green's function, which is the  $q$ -th component of the particle velocity at station  $\mathbf{x}_B$  due to a unit force source in the  $p$ -th direction at station  $\mathbf{x}_A$ .  $S(t)$  is the auto-correlation of the noise source time function.  $\langle \rangle$  means the ensemble average. The cross-correlation  $C_{qp}^{vel}(\mathbf{x}_B, \mathbf{x}_A, t)$  between two stations is defined as

$$C_{qp}^{vel}(\mathbf{x}_B, \mathbf{x}_A, t) = \frac{1}{T} \int_0^T v_p(\mathbf{x}_A, \tau) v_q(\mathbf{x}_B, \tau + t) d\tau, \quad (2)$$

where  $v_i(\mathbf{x}, t)$  is the  $i$ -th component of the ground velocity observed at station  $\mathbf{x}$ , and  $T$  is the window length for the time series. In the frequency domain, eq. (1) becomes

$$\langle v_p^*(\mathbf{x}_B, \mathbf{x}_A, \omega) v_q(\mathbf{x}_B, \mathbf{x}_A, \omega) \rangle \approx 2\Re \left\{ \dot{G}_{qp}(\mathbf{x}_B, \mathbf{x}_A, \omega) \right\} \mathcal{S}(\omega), \quad (3)$$

where  $\omega$  is the angular frequency, and  $*$  is complex conjugate. We use the time-domain representation in our analysis.

### Data set and data processing

Figure 1 shows the distribution of 24 F-net broadband seismic stations in southwestern Japan used in this study, which are installed and operated by the National Research Institute for Earth Science and Disaster Prevention (NIED). Those F-net broadband seismic stations have the Streckeisen STS-1 and STS-2 broadband sensors. The seismic data are digitized to 27 bit data with a sampling frequency of 100 Hz (Okada *et al.*, 2004).

The yearly continuous data from September 2008 to August 2009 are divided into 8,760 hourly segments. The segments containing instrumental troubles and data lost are rejected according to the data acquisition trouble log on the F-net Web site. Each segment is band-pass filtered between 0.02 and 10 Hz after removing the mean. Then, temporal normalization is applied to the data to reduce the effects on cross-correlations of earthquakes, instrumental irregularities, and local non-stationary noise source around the stations. This procedure is very important to increase the signal-to-noise ratio in the estimated interstation Green's functions. Here, we adopt a one-bit normalization technique as the temporal normalization, which has been used in a number of previous papers (e.g., Shapiro and Campillo, 2004; Sabra *et al.*, 2005). After preparing hourly time series data for each individual station, the cross-correlations of data for 211 station-to-station pairs whose interstation distance are less than 400 km are computed in the time-domain according to the equation (2). Finally all the hourly cross-correlations are stacked over a year.

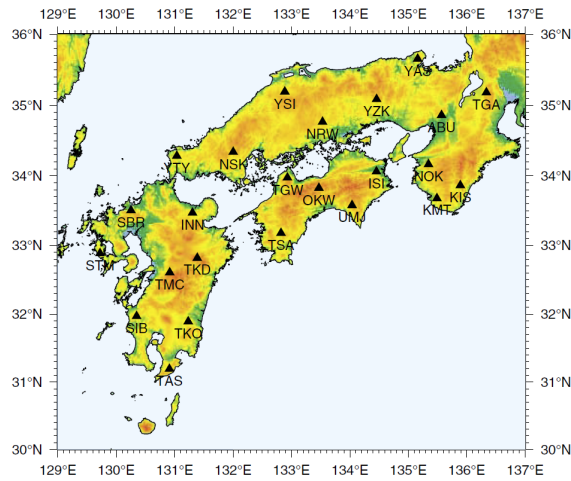


Fig. 1. Map of the F-net broadband seismic stations used for extracting interstation Green's functions.

### Examples of estimated interstation Green's functions

Since the seasonal dependence of the obtained cross-correlations of wavefields in this region was reported (Yamashita *et al.*, 2010), we use a year-long data set to suppress the effect of seasonal change in the predominant noise source during a year. Figure 2 shows the monthly cross-correlations of data between YSI and UMJ. Its interstation distance is 208 km. The clear coherent signals propagating from YSI to UMJ (positive time lag) are predominant in the winter season, and those propagating from UMJ to YSI (negative time lag) are predominant in the summer season. The 1 yr cross-correlation exhibits a temporal symmetry as expected from the theory.

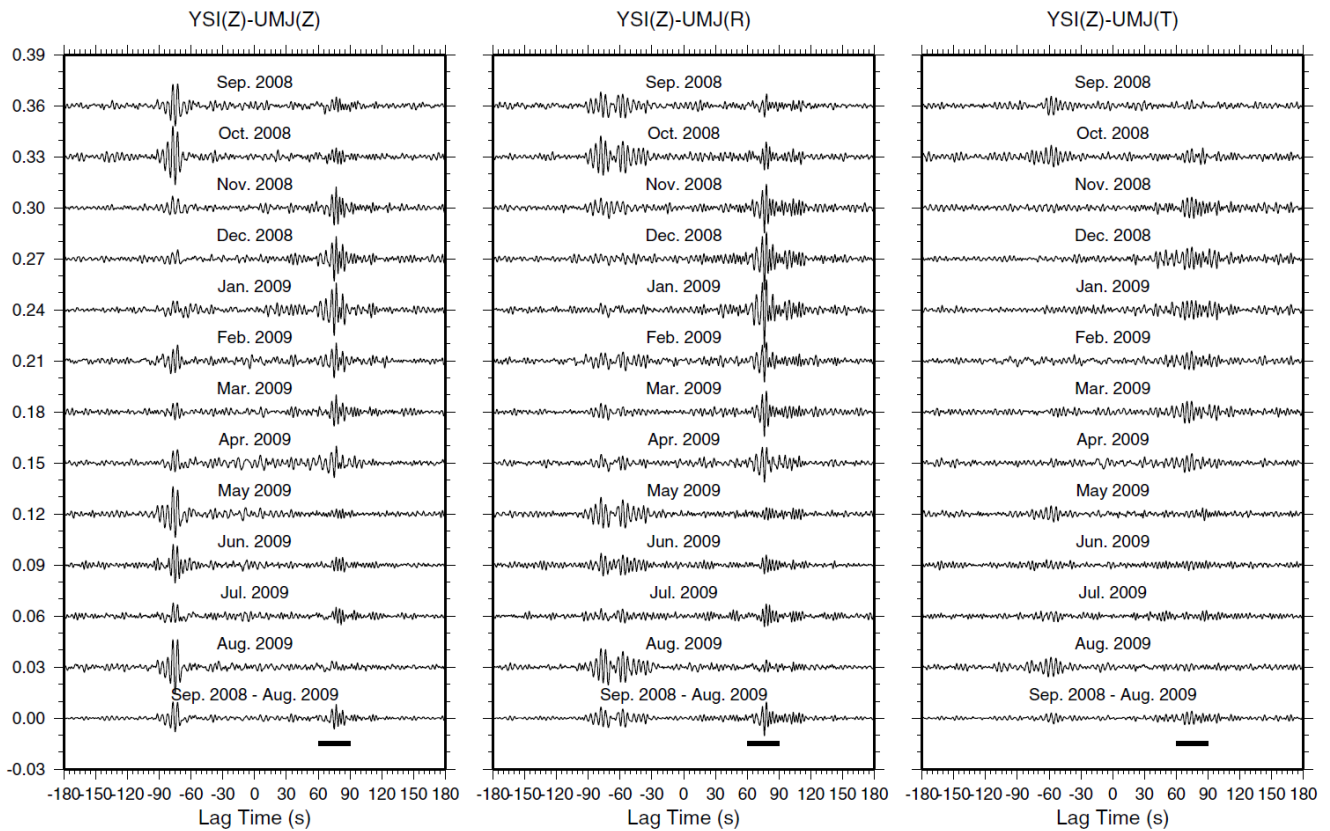


Fig. 2. Monthly and yearly cross-correlation functions for the station pair YSI and UMJ. The stacked cross-correlations between the vertical (Z) component at YSI and the vertical (Z), radial (R), and transverse (T) components at UMJ are shown.

Figure 3 shows the particle motion of the interstation Green's function from YSI to UMJ, which has been obtained from the yearly stacked cross-correlation function in the time window (60–90 s) indicated by the bars in Fig. 2, where the most predominant signal emerged. The observed particle motion shows a retrograde motion restricted within the propagation plane, which is a typical characteristic of a Rayleigh wave propagating at the free surface. That is, the predominant signal in the obtained interstation Green's function is concluded to be Rayleigh waves propagating from YSI to UMJ.

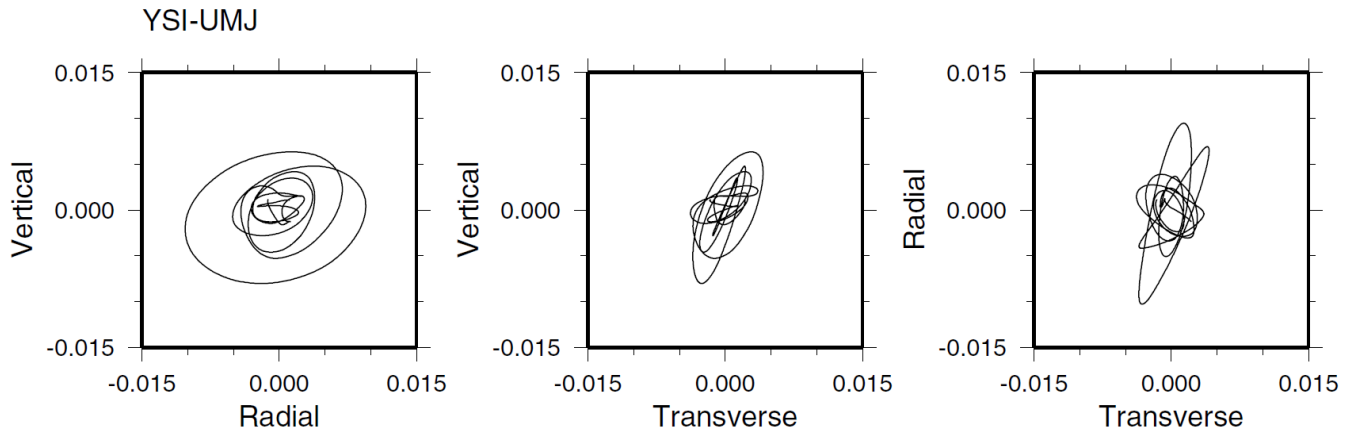


Fig. 3. Particle motion in the time window indicated by the bar in Fig. 2.

Figure 4 is the plots of the vertical component of interstation Green's functions due to the vertical single force ( $Z-Z$ ) for all station-to-station pairs as a record section with respect to the interstation distance. The clear propagating signals could be recognized for both positive and negative correlation lags up to the interstation distance of about 400 km from this plot. From the predominant period in the observed cross-correlation functions, these surface waves are thought to be originated by microseism.

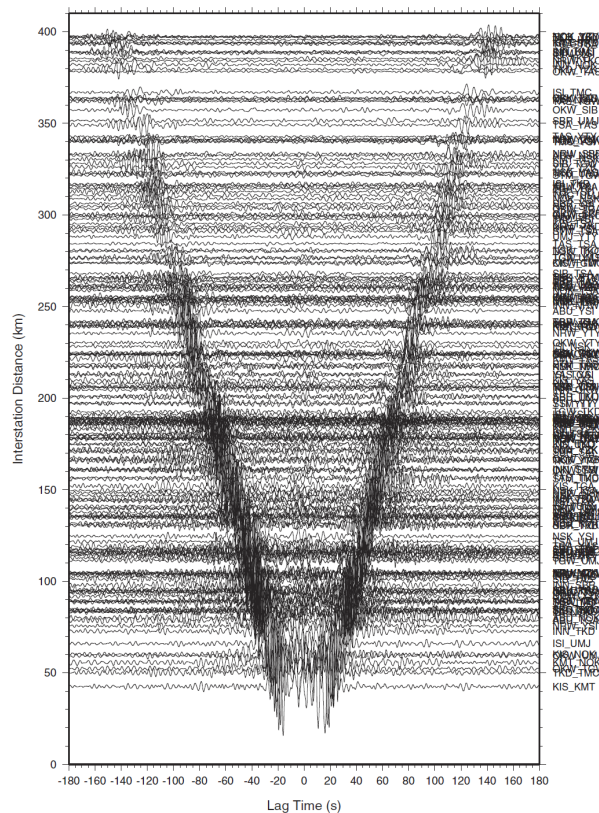


Fig. 4. Record section of cross-correlation functions with respect to the interstation distance.

## ESTIMATION OF RAYLEIGH WAVE GROUP VELOCITY ALONG PATH

The average Rayleigh wave group velocity along the propagation path of each station-to-station pair is estimated by the multiple filter analysis by Dziewonski *et al.* [1969]. In Fig. 5, the estimated group velocities for each station-to-station pair are shown on the map at periods of 2.8, 4.1, 6.1, and 7.9 s. Clear normal dispersion characteristics of group velocities could be recognized from this figure. At periods of 4.1, 6.1, and 7.9 s, the estimated group velocities along the paths across the north part of the studied area appears to be faster than those along the path across the south part of the studied area. This difference might suggest thinner surface low-velocity layer or faster *S*-wave velocity in the crust.

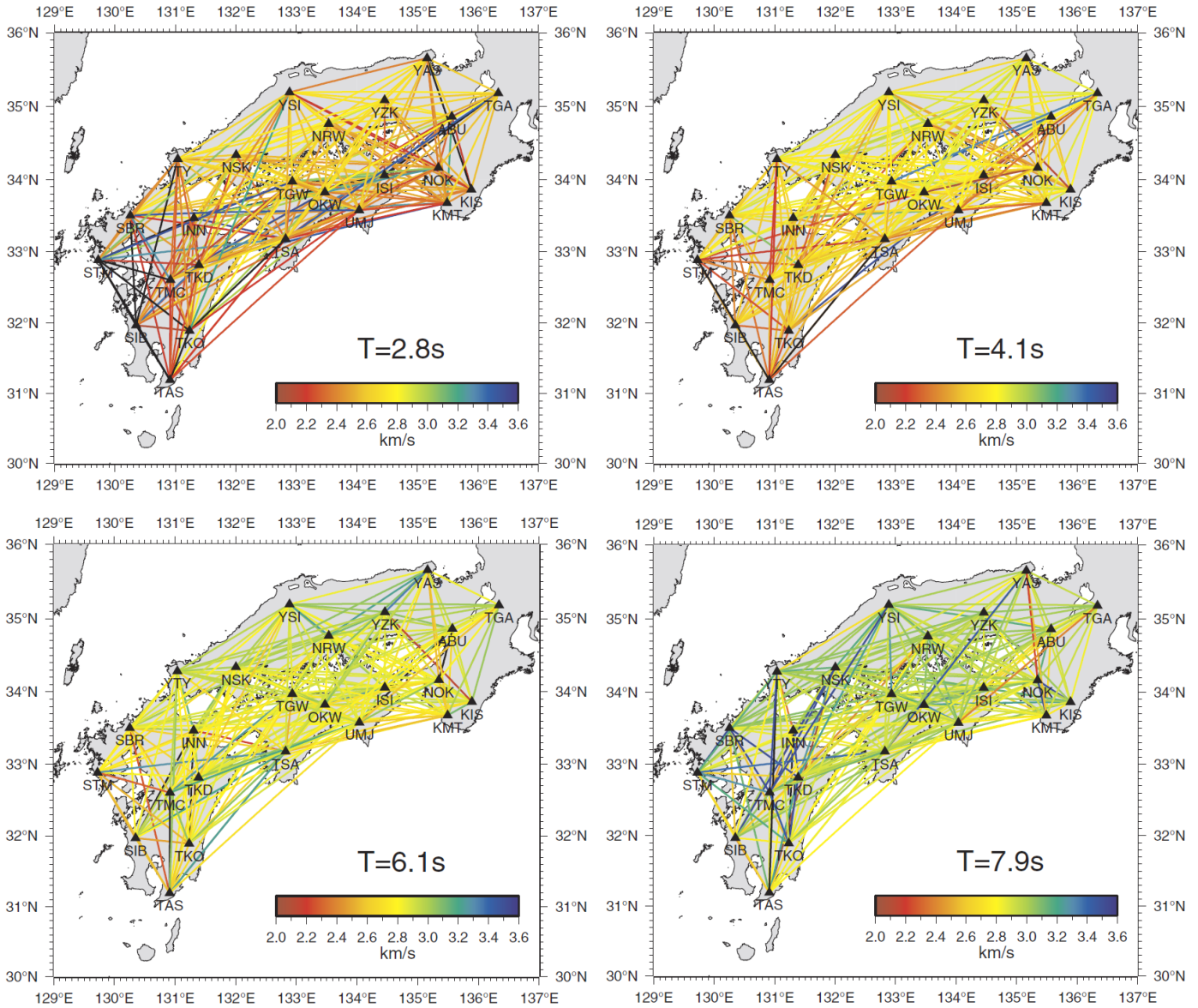


Fig. 5. Map showing the estimated group velocities at periods of 2.8, 4.1, 6.1, and 7.9 s.

## COMPARISON WITH SYNTHETIC GREEN'S FUNCTIONS

The three-dimensional crustal velocity structure model by Iwata *et al.* [2008] introduced in a previous section is composed of nine layers with constant values of *P*- and *S*-wave velocities, density, and quality factor *Q* within each layer. The geometry of each model



interface is defined by the 2-D B-spline function (Fig. 6). To build the model, they compiled velocity profiles from various seismic survey results. They used the OBS velocity models in offshore areas for the accretion prism (sedimentary wedge) and the oceanic crust, seismicity data for the seismogenic slab and the upper crust, receiver function inversion results for Moho, Conrad and slab, deep seismic profiles from refraction and wide-angle reflection explorations for inland areas, and generalized seismic tomography results. Material parameters ( $V_p$ ,  $V_s$ , density  $\rho$ , and  $Q$  value) of their model are listed in Table 1 (Model 0). The surface low-velocity layer, upper crust, lower crust, and mantle wedge belong to the continental plate (Eurasian plate), and the oceanic crust, slab, and upper mantle belong to the oceanic plate (Philippines Sea Plate). The schematic cross section can be found in Fig. 2 of Iwata *et al.* [2008]. The oceanic sedimentary layer (accretion prism) with the  $S$ -wave velocity of 1.0 km/s is neglected in this simulation because we are now interested in the wave propagation on the continental crust and want to reduce the computational load. Of course, this oceanic sedimentary layer is quite important in ground motion simulations for subduction events as pointed by Yamada and Iwata [2005].

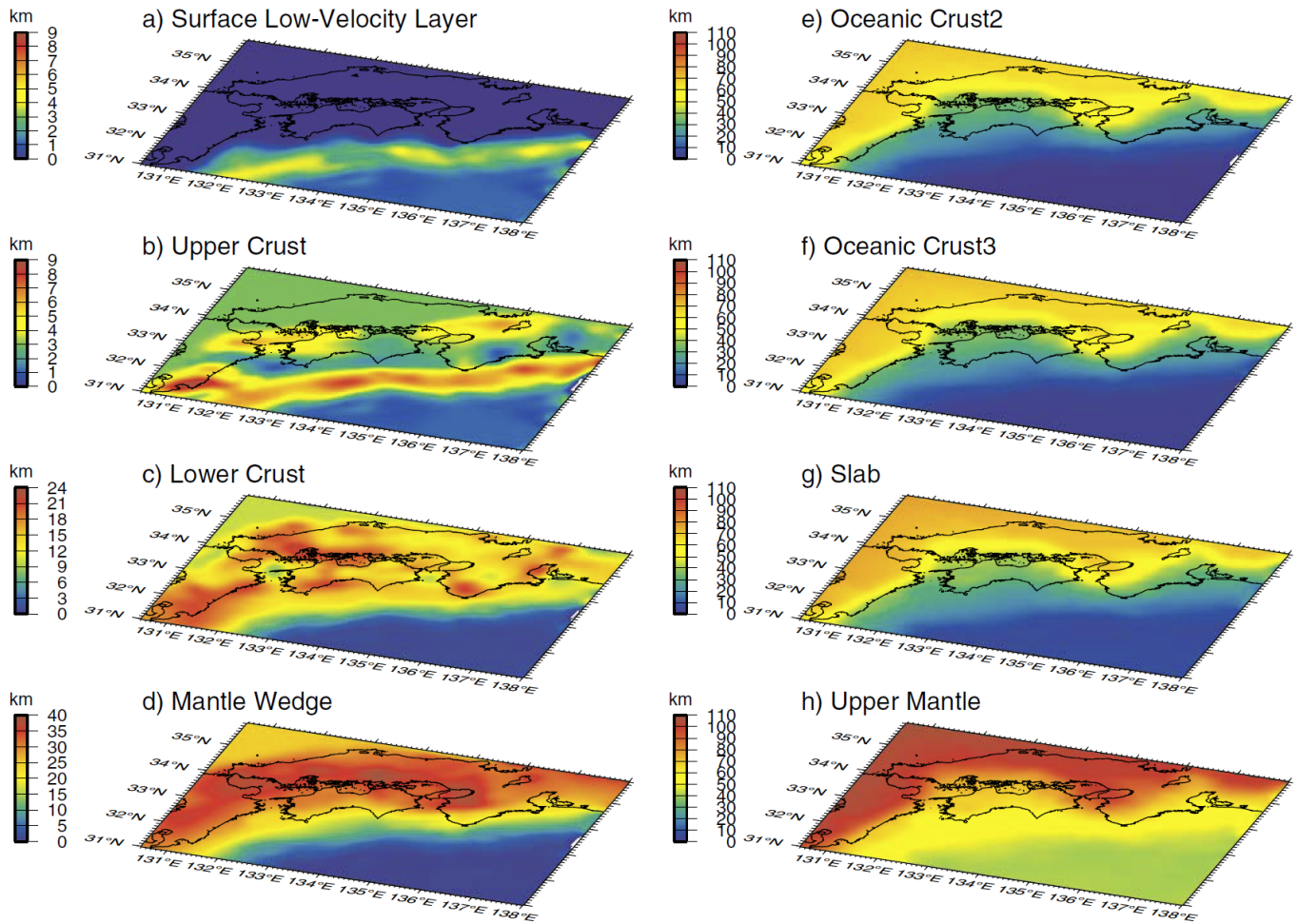


Fig. 6. Surface depth of each layer in the crustal velocity structure model by Iwata *et al.* (2008).

The synthetic Green's function in the three-dimensional velocity structure (Iwata *et al.*, 2008) excited by a vertical single force on the Earth's surface are computed by the finite difference method using the code developed by Pitarka [1999]. Our FDM model space occupies a 640 km  $\times$  520 km area of southwestern Japan and it extends to a depth of 80 km below Tokyo Peil (T.P.). The grid spacing is 0.5 km along the horizontal and vertical axes. The minimum  $S$ -wave velocity of the original model is 2.7 km/s. The reference period of  $Q$  model is 3.0 s. Since the elevation of most broadband stations is smaller than the grid size, this simulation does not consider the surface topographic effect.

In this simulation, a vertical single force is applied at station YSI (solid triangle in Fig. 6(a)), and three-dimensional wave propagation is solved for 180 s after the origin time. Figures 7 and 8 show the result of the simulation, and compared with the observed interstation Green's functions obtained in this study for two frequency bands (0.1–0.2 Hz and 0.2–0.33 Hz). The main wave packets in the theoretical Green's functions calculated from the Model 0 show systematically later arrival than those in the observation for most

stations in this region. We made additional ground motion simulation by changing the  $P$ - and  $S$ - wave velocities at the surface low-velocity layer (Models 1 and 2). The Model 1 changes only the  $S$ -wave velocity to make  $V_P/V_S$  be 1.73. The Model 2 gives higher  $P$ - and  $S$ - wave velocities according to the previous study by Iwaki *et al.* [2009], in which they determined the  $P$ - and  $S$ - wave velocities at the bedrock for the ground motion simulation in the Oita plain for the 2000 Tottori earthquake by trial and error to fit the observation. It looks that Model 2 gives better waveform fitting at most stations except some stations where the simulation using Model 1 seems to be better. We will make more comparison of waveforms for other source locations in the same way to see the general performance of the models.

Table 1. Model Parameters of the Crustal Velocity Structure Models Considered

Layer	Model 0		Model 1		Model 2		Common to Models 0~2	
	$V_P$ (km/s)	$V_S$ (km/s)	$V_P$ (km/s)	$V_S$ (km/s)	$V_P$ (km/s)	$V_S$ (km/s)	$\rho$ (g/cm <sup>3</sup> )	$Q$
Surface low-velocity layer	5.00	2.70	5.00	2.90	5.50	3.20	2.70	500
Upper crust	6.00	3.45	6.00	3.45	6.00	3.45	2.80	1000
Lower crust	6.70	3.90	6.70	3.90	6.70	3.90	2.90	500
Mantle wedge	7.70	4.45	7.70	4.45	7.70	4.45	3.10	1000
Oceanic crust layer 2	6.00	3.45	6.00	3.45	6.00	3.45	2.70	500
Oceanic crust layer 3	6.70	3.90	6.70	3.90	6.70	3.90	2.80	500
Slab	8.00	4.63	8.00	4.63	8.00	4.63	3.22	1000
Upper mantle	7.90	4.57	7.90	4.57	7.90	4.57	3.10	1000

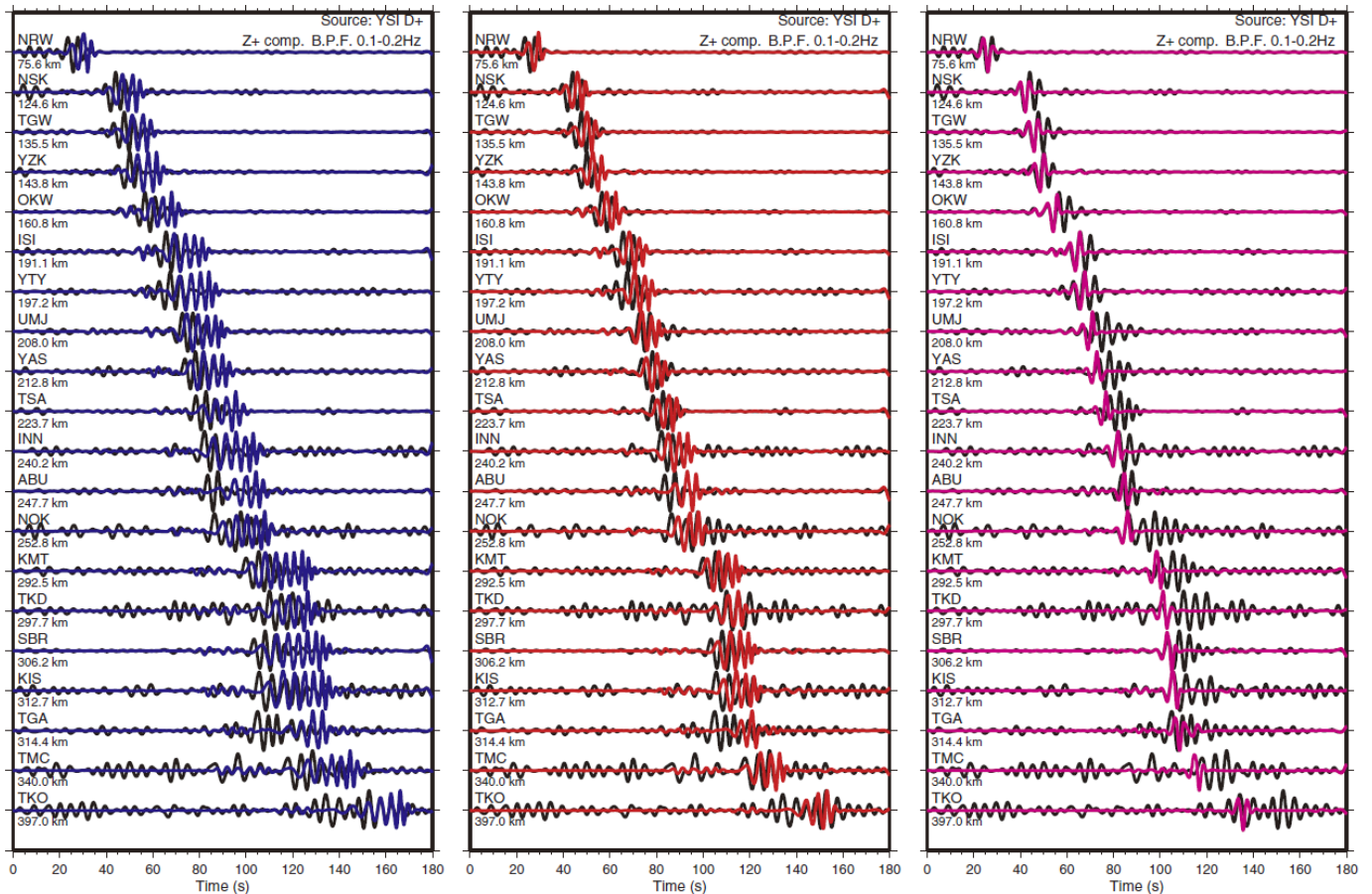


Fig. 7. Comparison of the vertical velocity Green's functions due to a vertical force at YSI from observations (black) with FDM simulations (blue for Model 0, red for Model 1, and magenta for Model 2) in the frequency band between 0.1 and 0.2 Hz.

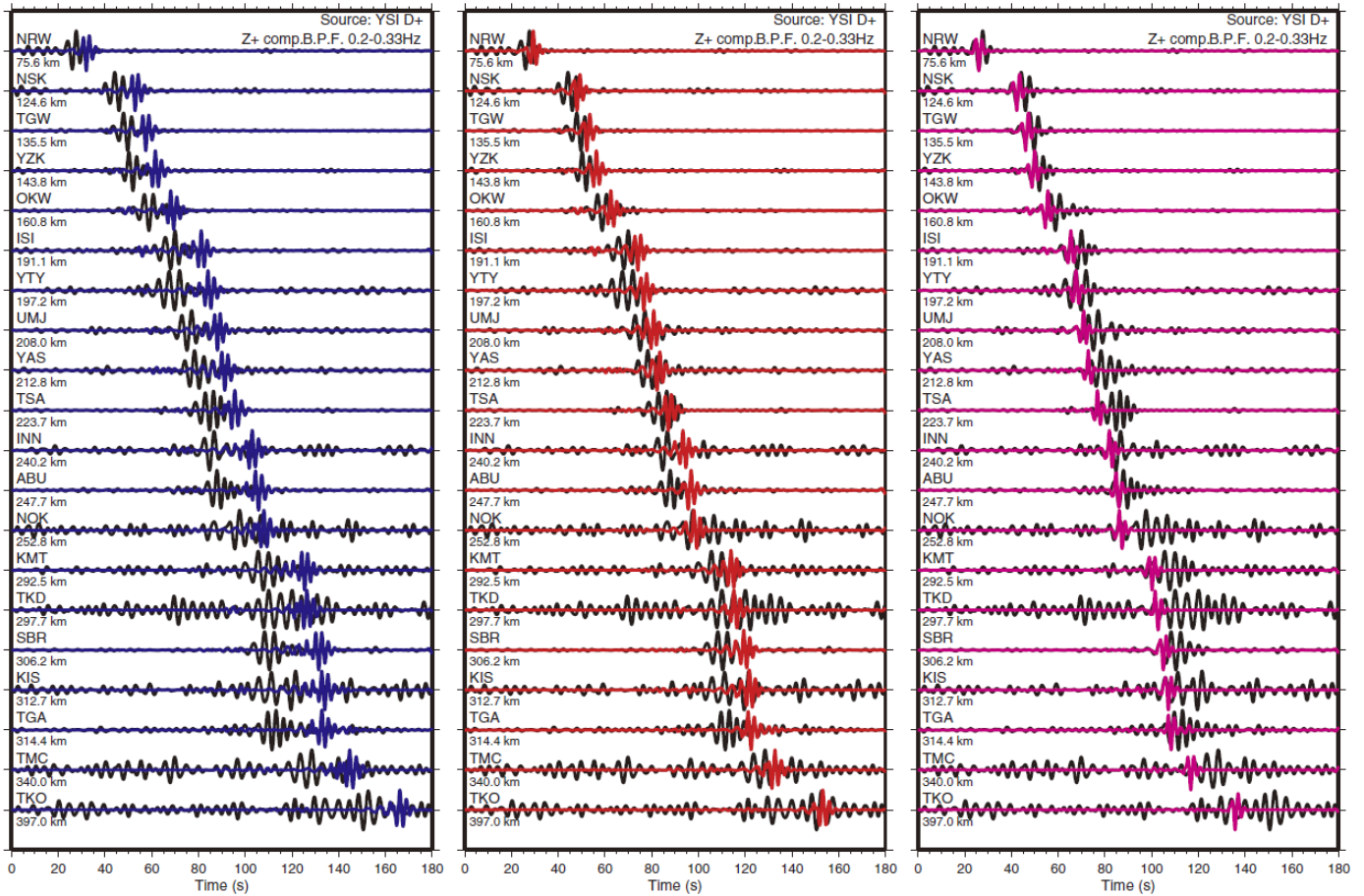


Fig. 8. Comparison of the vertical velocity Green's functions due to a vertical force at YSI from observations (black) with FDM simulations (blue for Model 0, red for Model 1, and magenta for Model 2) in the frequency band between 0.2 and 0.33 Hz.

## CONCLUSIONS

Interstation Green's functions are estimated for 211 paths in the long-period range (2–10 s) by correlating the yearly continuous records from 24 broadband seismic stations in southwestern Japan. The signals which propagate on the ground surface with the characteristics of Rayleigh wave emerged from the ambient seismic noise field. In Chugoku region the estimated group velocity was faster than Shikoku region, which showed the possibility of the difference in the shear-wave velocity or the thickness of the surface layer between these regions. The observed interstation Green's functions were compared with the theoretical Green's functions calculated using the three-dimensional crustal velocity model by the finite difference method. They suggested that higher  $P$ - and  $S$ -wave velocities at the surface layer are expected to explain the travel time and waveforms of the observed interstation Green's functions. This study also illustrated that the seismic interferometry technique is a useful tool in ground motion prediction studies.

## ACKNOWLEDGMENTS

The continuous broadband seismic data from F-net broadband network operated by NIED are used in this study. Part of initial data processing was helped by Kaori Yamashita.

## REFERENCES

Bensen, G. D., M. H. Ritzwoller, M. P. Barmin, A. L. Levshin, F. Lin, M. P. Moschetti, N. M. Shapiro, and Y. Yang [2007], "Processing Seismic Ambient Noise Data to Obtain Reliable Broad-band Surface Wave Dispersion Measurements", *Geophys. J. Int.*,



Vol. 169, No. 3, pp. 1239-1260.

Campillo, M., and A. Paul [2003], “Long Range Correlations in the Seismic Coda”, *Science*, Vol. 299, No. 5606, pp. 547-549.

Dziewonski, A., S. Bloch, and M. Landisman [1969], “A Technique for the Analysis of Transient Seismic Signals”, *Bull. Seism. Soc. Am.*, Vol. 59, No. 1, pp. 427-444.

Headquarters for Earthquake Research Promotion [2011], “Evaluation of Major Subduction-zone Earthquakes”, <http://www.jishin.go.jp/main/index-e.html>.

Iwaki, A., T. Iwata, H. Sekiguchi, K. Asano, M. Yoshimi, and H. Suzuki [2009], “Simulation of Long-period Ground Motion in Oita Plain due to a Hypothetical Nankai Earthquake”, *Zisin 2 (J. Seismol. Soc. Jpn.)*, Vol. 61, No. 4, pp. 161-173 (in Japanese with English abstract).

Iwata, T., T. Kagawa, A. Petukhin, and Y. Ohnishi [2008], “Basin and Crustal Velocity Structure Models for the Simulation of Strong Ground Motions in the Kinki Area, Japan”, *J. Seismol.*, Vol. 12, No. 2, pp. 223-234.

Ma, S., G. A. Prieto, and G. C. Beroza [2008], “Testing Community Velocity Models for Southern California Using the Ambient Seismic Field”, *Bull. Seism. Soc. Am.*, Vol. 98, No. 6, pp. 2694-2714.

Okada, Y., K. Kasahara, S. Hori, K. Obara, S. Sekiguchi, H. Fujiwara, and A. Yamamoto [2004], “Recent progress of seismic observation networks in Japan –Hi-net, F-net, K-NET and KiK-net–”, *Earth Planets Space*, Vol. 56, No. 8, pp. xv-xxviii.

Pitarka, A. [1999], “3D Elastic Finite-Difference Modeling of Seismic Motion Using Staggered Grids with Nonuniform Spacing”, *Bull. Seism. Soc. Am.*, Vol. 89, No. 1, pp. 54-68.

Sabra, K. G., P. Gerstoft, P. Roux, W. A. Kuperman, and M. C. Fehler [2005], “Extracting Time-Domain Green’s Function Estimates from Ambient Seismic Noise”, *Geophys. Res. Lett.*, Vol. 32, No. 3, L03310, doi: 10.1029/2004GL021862.

Shapiro, N. M., and M. Campillo [2004], “Emergence of Broadband Rayleigh Waves from Correlations of the Ambient Seismic Noise”, *Geophys. Res. Lett.*, Vol. 31, No. 7, L07614, doi: 10.1029/2004GL019491.

Snieder, R. [2004], “Extracting the Green’s Function from the Correlation of Coda Waves: A Derivation Based on Stationary Phase”, *Phys. Rev. E*, Vol. 69, No. 4, 046610.

Wapenaar, K., and J. Fokkema [2006], “Green’s function representations for seismic interferometry”, *Geophysics*, Vol. 71, No. 4, pp. SI33-SI46.

Yamada, N., and T. Iwata [2005], “Long-period ground motion simulation in the Kinki area during the  $M_j$  7.1 foreshock of the 2004 off the Kii peninsula earthquake”, *Earth Planets Space*, Vol. 57, No. 3, pp. 197-202.

Yamanaka, H., K. Chimoto, T. Moroi, T. Ikeura, K. Koketsu, M. Sakaue, S. Nakai, T. Sekiguchi, and Y. Oda [2010], “Estimation of Surface-wave Group Velocity in the Southern Kanto Area Using Seismic Interferometric Processing of Continuous Microtremor Data”, *BUTSURI-TANSA (Explor. Geophys.)*, Vol. 63, No. 5, pp. 409-425 (in Japanese with English abstract).

Yamashita, K., K. Asano, and T. Iwata [2010], “Crustal Velocity Structure in Western Japan Using Seismic Interferometry (1) Estimation of Surface Wave Group Velocity”, *Annuals of Disas. Prev. Res. Inst., Kyoto Univ.*, No. 53B, pp. 175-180 (in Japanese).